BIOCHEMISTRY
including biophysical chemistry & molecular biology

Article

pubs.acs.org/biochemistry

Key Chemical Factors of Arginine Finger Catalysis of F_1-ATPase Clarified by an Unnatural Amino Acid Mutation

Ayako Yukawa,[†] Ryota Iino,[‡,§] Rikiya Watanabe,[†,∥,⊥] Shigehiko Hayashi,[#] and Hiroyuki Noji*[,†,∥]

[†]Department of Applied Chemistry, Graduate School of Engineering, The University of Tokyo, Tokyo 113-8656, Japan

[‡]Okazaki Institute for Integrative Bioscience, Institute for Molecular Science, National Institutes of Natural Sciences, Okazaki, Aichi 444-8787, Japan

[§]Department of Functional Molecular Science, School of Physical Sciences, The Graduate University for Advanced Studies (SOKENDAI), Hayama, Kanagawa 240-0193, Japan

[∥]CREST, Japan Science and Technology Agency (JST), Tokyo 113-8656, Japan

[⊥]PRESTO, Japan Science and Technology Agency (JST), Tokyo 113-8656, Japan

[#]Department of Chemistry, Graduate School of Science, Kyoto University, Kyoto 606-8502, Japan

Supporting Information

ABSTRACT: A catalytically important arginine, called Arg finger, is employed in many enzymes to regulate their functions through enzymatic hydrolysis of nucleotide triphosphates. F_1-ATPase (F_1), a rotary motor protein, possesses Arg fingers which catalyze hydrolysis of adenosine triphosphate (ATP) for efficient chemomechanical energy conversion. In this study, we examined the Arg finger catalysis by single-molecule measurements for a mutant of F_1 in which the Arg finger is substituted with an unnatural amino acid of a lysine analogue, 2,7-diaminoheptanoic acid (Lyk). The use of Lyk, of which the side chain is elongated by one CH_2 unit so that its chain length to the terminal nitrogen of amine is set to be equal to that of arginine, allowed us to resolve key chemical factors in the Arg finger catalysis, i.e., chain length matching and chemical properties of the terminal groups. Rate measurements by single-molecule observations showed that the chain length matching of the side-chain length is not a sole requirement for the Arg finger to catalyze the ATP hydrolysis reaction step, indicating the crucial importance of chemical properties of the terminal guanidinium group in the Arg finger catalysis. On the other hand, the Lyk mutation prevented severe formation of an ADP inhibited state observed for a lysine mutant and even improved the avoidance of inhibition compared with the wild-type F_1. The present study demonstrated that incorporation of unnatural amino acids can widely extend with its high "chemical" resolution biochemical approaches for elucidation of the molecular mechanism of protein functions and furnishing novel characteristics.

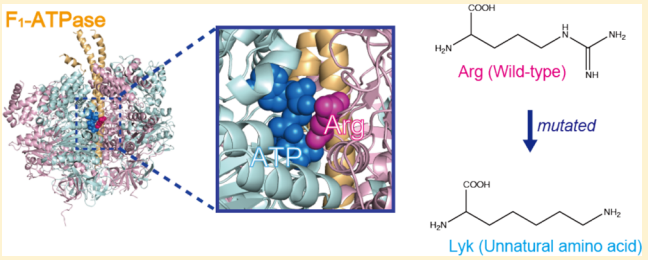

Chemical reactions of hydrolysis and phosphate transfer of nucleotide triphosphate (NTP) are utilized in diverse biological processes such as metabolism, mechanical movement and transport, and signaling. Enzymes that catalyze chemical reactions of NTP control the catalytic activity, realizing coupling of the reactions with their biological functions. Many of such enzymes of NTP reactions employ a catalytic arginine residue called the arginine (Arg) finger[1−12] for control of the catalytic activity.

Molecular mechanism of catalytic regulation by Arg finger is, however, still unclear. Theoretical investigations[13−18] have revealed that electrostatic interaction given by coordination of a positively charged guanidinium group of Arg finger to NTP stabilizes its electronic structure in the reaction transition state. The role of electrostatic interaction well explains that a lysine residue, which also carries a positive charge at its terminal amine group, has also been suggested to serve as a catalytic residue for hydrolysis of adenosine triphosphate (ATP) in some ATPases such as RecA.[11,12] However, simple replacement of Arg finger with lysine in NTPs drastically retards its catalytic activity,[1,19] indicating that control of catalysis by Arg finger requires fine-tuning of its coordination to NTP.

Chemical features of arginine and lysine that differentiate the catalytic activity remain elusive since many chemical differences between those residues still exist despite that both of the terminal groups carry a positive charge. One difference is their side-chain length. The number of carbon atoms up to the terminal nitrogen in the side chain of lysine is fewer by one than that of carbon and nitrogen atoms of arginine so that the length of the side chain of lysine to the nitrogen of the terminal amine group is about 1 Å shorter than that of arginine to one of the terminal nitrogens. As positional rearrangement of the Arg

Received: September 10, 2014
Revised: December 9, 2014
Published: December 22, 2014

DOI: 10.1021/bi501138b
Biochemistry 2015, 54, 472−480

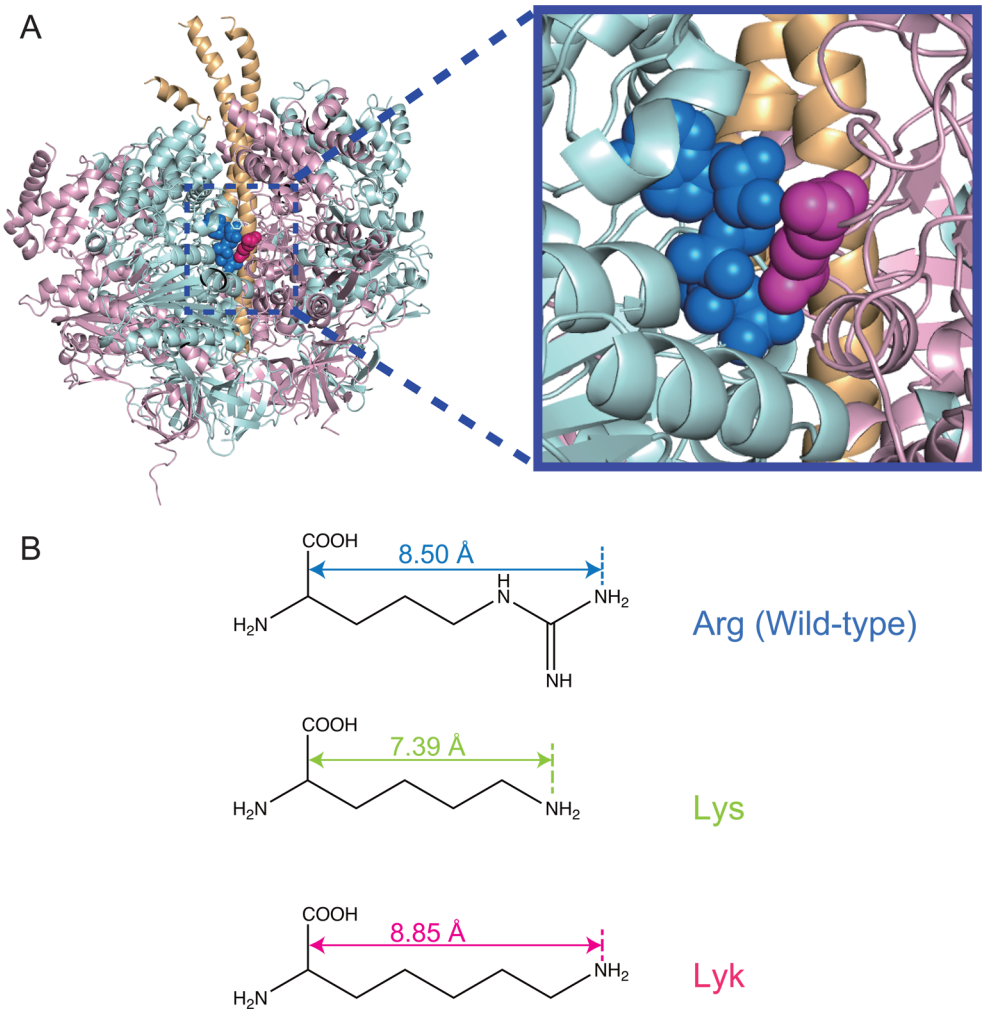

Figure 1. Position of the arginine finger and chemical structures of the amino acid residues. A, crystal structure of mitochondrial F_1 (MF_1) viewed from the side, β_{DP}/α_{DP} catalytic interface (PDB code 1BMF). The α, β, and γ subunits are shown in pearl pink, pearl blue, and pearl yellow, respectively. The "arginine finger" in the α subunit (αR373 in MF_1) is shown by pink space-filling model. AMP-PNP bound to the catalytic site are shown by blue space-filling model. B, chemical structures and side-chain length of arginine (Arg, top), lysine (Lys, middle), and 2,7-diaminoheptanoic acid (Lyk, bottom). The arginine finger of TF_1, αR364, was mutated into Lyk (αR364Lyk) in this study.

finger is expected to be involved for control of catalytic activity in functional processes,[2,20] the difference in length to the nitrogens which coordinate to the substrate is possibly a key factor.

Furthermore, obviously, chemical structures of their terminal groups are different. The guanidinium group of arginine possesses a planarly extended structure, giving rise to strongly anisotropic electrostatic interaction with its surrounding environment. The planarity and heterogeneous charge distributions originating from conjugated electronic structure lead to weak out-of-plane and strong in-plane electrostatic interactions. The amphiphilic character is suggested to contribute to formation of like-charge Arg-Arg stacking pairs in water[21−26] and at interfaces of oligomeric proteins.[27] In contrast, the amine group of lysine exhibits localized distribution of a positive charge and thus results in stronger and more isotropic interaction with the surroundings. It is, however, rather difficult to resolve the chemical details that determine the catalytic activity through a conventional biochemical approach.

In the present study, we focus on Arg finger catalysis in F_1, which is the water-soluble portion of the F_oF_1-ATP synthase and acts as an ATP-driven rotary molecular motor.[28−30] Bacterial F_1 is composed of $\alpha_3\beta_3\gamma\delta\varepsilon$ subunits and the minimum complex as a motor is the $\alpha_3\beta_3\gamma$ subcomplex.[31] The $\alpha_3\beta_3$ forms the stator ring, and the γ subunit is the rotary shaft.[4,32,33] Three catalytic sites reside at the three $\alpha-\beta$ interfaces, mainly on the β subunits;[4,32,33] i.e., F_1 possesses three catalytic sites.[31,34−36] The rotary mechanism of F_1 has been well studied in the single-molecule rotation assays. Upon ATP hydrolysis, F_1 rotates in the anticlockwise direction, hydrolyzing three molecules of ATP during one γ rotation.[37] Due to the tight chemo-mechanical coupling, the rotational rate of F_1 is one-third of the ATP hydrolysis rate, which can be described as a simple Michaelis−Menten kinetics.[37] F_1 generates a rotary torque of 40 pN·nm·rad^{-1} upon rotation.[38,39] The work per one γ rotation is thus estimated as 240 pN·nm, which is balanced by the hydrolysis of three ATP molecules. Therefore, F_1 is extremely efficient in converting chemical energy to mechanical work, which is the prominent feature of F_1 among ATP-driven motor proteins. An elementary step size of the rotation is 120°, each of which is coupled with a single turnover of ATP hydrolysis.[38] The 120° step can be further resolved into 80° and 40° substeps, each triggered by ATP binding/ADP release

DOI: 10.1021/bi501138b
Biochemistry 2015, 54, 472−480

and ATP cleavage/P_i release.[36,37] The pauses before the 80° and 40° substeps are referred to as the binding dwell and the catalytic dwell, respectively.

To clarify how Arg fingers of F_1 contribute to the catalysis in detail, various studies have been done as follows; Several biochemical and X-ray crystallographic studies[5−7,20] revealed that Arg fingers located in the α subunits (Figure 1A), αR373 in mitochondrial F_1 (MF_1) and αR364 in the thermophilic F_1, as well as residues forming the catalytic site in the β subunits play a crucial role in the catalysis. A single-molecule experiment found that substitution of the Arg finger with lysine largely reduces the catalytic activity by 280.[19] A recent work showed that even when F_1 loses the positive charge, F_1 still retains catalytic power.[40] However, the catalytic activity was decreased by the factor of 2,400 suggesting the critical role of Arg finger in rate enhancement of catalysis.

In order to identify chemical determinants of the Arg finger catalysis, we introduced an unnatural amino acid, 2,7-diaminoheptanoic acid (hereafter referred to as Lyk), substituting the Arg finger. Lyk is a lysine analogue with an alkyl chain elongated by one CH_2 unit (Figure 1B). The elongation sets the length of the side chain of Lyk to be equal to that of arginine, eliminating the difference in chain length between arginine and lysine, while their chemical groups remained different. Thus, kinetics measurement of a Lyk mutant enables one to identify the chemical determinants that create a difference between arginine and lysine, i.e., the chain length or the terminal chemical group, in the catalysis. We successfully reconstituted the mutant of $\alpha_3\beta_3\gamma$ complex with α subunits including the unnatural amino acids using an *Escherichia coli* (*E. coli*) cell-free protein expression system. Through measurement with a single-molecule rotational assay, which allows one to resolve elementary steps of ligand binding/release and catalytic reaction involved in the complex motor process, key factors of the Arg finger for the rotary catalysis of F_1 were identified in detail; i.e., we discovered that chemical properties of the terminal groups are crucial for efficient catalysis of ATP and side-chain length matching contributes to the avoidance of inhibition-states formation.

EXPERIMENTAL PROCEDURES

Preparation of F_1(αR364Lyk). A mutant α(His_6 at N-terminus/FLAG-tag at C-terminus/C193S/R364Lyk) subunit (referred to as αR364Lyk in this study for simplicity) of F_1 from thermophilic *Bacillus* PS3 was synthesized and purified using an *E. coli* cell-free protein expression system (Protein Express Corp., Miyoshi, Japan) (Figure S1). The amber suppressor tRNAs was used for substitution of the Arg finger at the 364th position of the α subunit with Lyk.[11] The mutant β(His_6 at N-terminus) and γ(S108C/I211C) subunits of F_1 from thermophilic *Bacillus* PS3, which were designed for rotation assay and are referred to as β and γ hereafter, were expressed together in *E. coli* JM103Δunc. Cells were cultured in Terrific Broth medium at 37 °C for at least 8 h and then harvested. Then, 40 μg of purified αR364Lyk dissolved in 40 μL of 100 mM KP_i (pH 7.0) and 2 mM ethylenediaminetetraacetic acid (EDTA) and crude extract of β and γ from 0.6 g of cells in 500 μL of 50 mM imidazole (pH 7.0) and 100 mM NaCl were mixed and incubated for 2 h in order to reconstitute the F_1 complex. Next, the mixture containing F_1(αR364Lyk) complex was mixed with Ni^{2+}-NTA agarose (Qiagen, Venlo, The Netherlands), which was equilibrated with 50 mM imidazole (pH 7.0) and 100 mM NaCl. After incubating for 1 h, the solution was centrifuged at 15000 rpm for 2 min; the supernatant was exchanged with 100 mM imidazole (pH 7.0) and 100 mM NaCl. This procedure was repeated several times, and finally the enzyme was eluted with 500 mM imidazole (pH 7.0) and 100 mM NaCl. The imidazole was removed by a NAP10 column (GE Healthcare, Pittsburgh, PA, USA). And, then, the purified F_1(αR364Lyk) was biotinylated as described previously.[28,41] During the entire purification process, the samples were treated at room temperature.

Rotation Assay of F_1(αR364Lyk). Rotation assay of F_1(αR364Lyk) was conducted by attaching a magnetic bead (0.2−0.4 μm; Seradyn, Indianapolis, IN, USA) to the γ subunit as the probe of rotation and immobilizing the $\alpha_3\beta_3$ ring on a Ni^{2+}-NTA coated coverglass with His-tags incorporated into the amino terminus of the α and β subunits. A flow chamber for the rotation assay was prepared as reported previously.[42] We used a phase-contrast microscope (IX-70; Olympus) with a 100× objective and recorded images at 30 or 1000 frames/s. All experiments were conducted at pH 7.

RESULTS

Rotation Assay of F_1(αR364Lyk). We observed rotation of F_1(αR364Lyk) by using magnetic beads as a rotation probe. F_1(αR364Lyk) showed successive and unidirectional rotations as the wild-type and F_1(αR364K) mutant (Figure 2A),[19] so that the mutant retained the catalytic activity. Next, we determined rotation rates of F_1(αR364Lyk) mutant at various ATP concentrations ranging from 10 nM to 50 mM. These values obeyed a simple Michaelis−Menten kinetics (Figure 2B, pink) as previously reported;[19,28] a maximum rotation rate (V_{max}) and a Michaelis constant (K_m) were 0.20 s^{-1} and 90 nM, respectively. Because V_{max} is apparently smaller than that of wild-type, some elementary reaction steps except for ATP binding, e.g., ATP cleavage or product release, limit the rotational rate of mutant F_1. Therefore, the catalytic rate constant for ATP hydrolysis (k_{cat}), which was determined from $3V_{max}$ assuming a coupling ratio of three ATPs per turn,[38] was 0.60 s^{-1}, and thus was found to be 5.1×10^2 times lower than that of the wild-type (303 s^{-1}). These values are almost equal to those derived from the dwell time analysis of the pauses at 1 mM ATP as shown below (see Figure 4B). In addition, the binding rate constant (k_{on}) for ATP determined from $3V_{max}/K_m$,[28] was 6.5×10^6 M^{-1} s^{-1}, which is only 3.4 times lower than that of the wild-type (2.2×10^7 M^{-1} s^{-1}). Two kinetic parameters, k_{cat} and k_{on}, of the wild-type, F_1(αR364Lyk) mutant, and F_1(αR364K) mutant are summarized in Table 1. These results indicate that the Lyk mutation significantly retards catalysis, while the effect of the mutation on ATP binding is minor.

Analyses of Stepping Rotation. F_1(αR364Lyk) mutant showed the discrete pauses even at saturating ATP concentrations (Figure 2A, inset), so that identification of the pausing angles allowed us to determine which pauses were derived from the binding dwell or the catalytic dwell. For this analysis, we conducted a buffer exchange experiment, in which the ATP concentration was reduced from 100 μM (saturating ATP concentration) to 100 nM ($\sim K_m$) during observation of rotating molecules (Figure 3A). At 100 nM ATP, three major peaks of the ATP binding dwell appeared at about +40° from the original pausing angles (Figure 3B). For statistical analysis, we compared the relative angular position of the original pauses ($\Delta\theta_1$) and that of the additional peaks which appeared at 100 nM ATP ($\Delta\theta_2$) before and after buffer exchange, whose

DOI: 10.1021/bi501138b
Biochemistry 2015, 54, 472−480

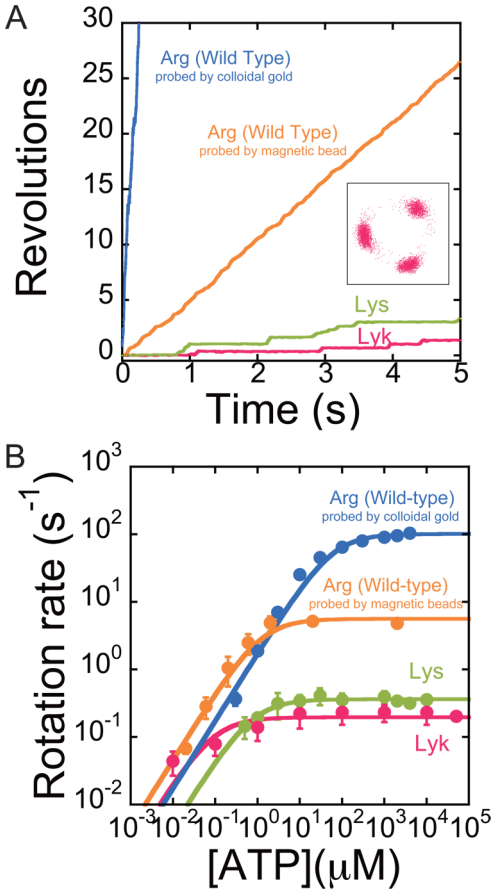

Figure 2. Time courses of rotation and kinetic analysis of wild-type, $F_1(\alpha R364K)$, and $F_1(\alpha R364Lyk)$. A, examples of the time courses of rotation at 1 mM ATP of the wild-type (blue) probed by colloidal gold (60 nm) and the wild-type (orange), $F_1(\alpha R364K)$ (green), and $F_1(\alpha R364Lyk)$ (pink) probed by magnetic beads (0.2−0.4-μm). B, rotation rate at various ATP concentrations of the wild-type (blue) probed by colloidal gold (60 nm) and the wild-type (orange), $F_1(\alpha R364K)$ (green), and $F_1(\alpha R364Lyk)$ (pink) probed by magnetic beads (0.2−0.4-μm). Error bars were determined from at least five different molecules. The data were fitted with the Michaelis−Menten equation, $v = V_{max}[ATP]/(K_m + [ATP])$. The values of V_{max}, K_m, and the calculated k_{on} ($3V_{max}/K_m$) are summarized in Table 1.

average values were −0.5 ± 8.5° and −39.2 ± 11.1° (N = 24 and 4 molecules), respectively (Figure 3C). Thus, we confirmed that $F_1(\alpha R364Lyk)$ pauses at the catalytic angle at saturated ATP concentrations. Furthermore, $F_1(\alpha R364Lyk)$ mutant sometimes lapsed into a long inactive state, i.e., the ADP inhibited state,[43] and resumed rotation again (Figure 3D). Then, the angular position during the ADP inhibited state was compared with that during the short pause (Figure 3E), and these two positions coincided with each other ($\Delta\theta$ = 0.0 ± 7.6°; N = 20 and 13 molecules; Figure 3F). Given that the wild-type F_1 lapses into the inhibited state at the catalytic angle,[43] this result also indicates that the angular position of the pause at saturating ATP concentration is the catalytic angle.

Identification of the Elementary Reaction Step That Causes Pauses at Saturating ATP Concentrations. The recently established reaction scheme of catalysis and rotation indicates that F_1 undergoes two reactions at the catalytic angle:[42] ATP cleavage step at the 200° state and inorganic phosphate (P_i) release step at the 320° state. Therefore, there are at least two possibilities for the reduction of the maximum rotation rate of $F_1(\alpha R364Lyk)$ mutant: slow ATP cleavage and/or slow P_i release. To clarify which elementary reaction step decelerates the rotation rate, we used an ATP analogue (adenosine 5-[γ-thio]-triphosphate, ATPγS), which retards the ATP cleavage step specifically by about 30-fold.[44] In the presence of ATPγS, $F_1(\alpha R364Lyk)$ mutant rotated much slower than that in the presence of ATP (Figure 4A). The distribution of dwell time at 1 mM ATPγS exponentially decayed with a time constant of 42 s (Figure 4B, bottom), which was 30 times longer than that at 1 mM ATP (1.4 s, Figure 4B, top). The proportion of the elongation of time constant by ATPγS was consistent with that observed for the wild-type F_1 between ATP and ATPγS.[44] This finding supports that the Lyk mutation retards the ATP cleavage step. In addition, we measured a rotation rate in the presence of P_i in solution and examined how P_i suppresses the rotation rate of $F_1(\alpha R364Lyk)$ (Figure 4C). Fitting with a curve according to a conventional competitive inhibition scheme yielded the inhibitory constant of 0.25 mM; the value was 4.9 times smaller than that of the wild-type (1.2 mM, Figure 4D). Considering that Lyk mutation suppressed V_{max} by a factor of 5.1 × 10^2, this effect on the rotation rate is minor. Thus, it is confirmed that the Lyk mutation mainly retards the ATP cleavage step.

Stiffness and Torque Measurement. In order to investigate effects of the Lyk mutation on the stability and robustness of the complex, we determined the stiffness of the $F_1(\alpha R364Lyk)$ using the equipartition theorem of energy, $(1/2)k_BT = (1/2)\kappa\sigma^2$, where k_B is the Boltzmann constant, T is absolute temperature, κ is the stiffness, and σ is the standard deviation of the angular position of the bead during the pause, respectively. The value of κ for $F_1(\alpha R364Lyk)$ was 54 pN·nm/rad and was 1.5 times smaller than that of the wild-type (79 pN·nm/rad, Figure 5A). Next, in order to investigate effects of the mutation on efficiency of the torque transmission, the torque of the $F_1(\alpha R364Lyk)$ mutant was measured with the method based on the fluctuation theorem,[39] which estimates the generated torque only from the rotation trajectory without assuming a frictional drag coefficient of a rotary probe. The torque of 29 pN·nm generated by $F_1(\alpha R364Lyk)$ mutant was 1.2 times smaller than that of the wild-type (37 pN·nm, Figure

Table 1. Kinetic Parameters of Wild-Type, $F_1(\alpha R364Lyk)$, and $F_1(\alpha R364K)$

sample	V_{max} (s^{-1})	K_m (M^{-1})	k_{on} (M^{-1} s^{-1})[a]	k_{cat} (s^{-1})[b]	ref
wild-type (colloidal gold)	101 ± 50[c]	(5.8 ± 4.5) × 10^{-5}	(2.2 ± 2.0) × 10^7	7.7 × 10^2	53
wild-type (magnetic beads)	5.6 ± 3.6	(1.2 ± 1.1) × 10^{-6}	(1.4 ± 1.6) × 10^7	ND[d]	this work
$F_1(\alpha R364Lyk)$ (magnetic beads)	0.20 ± 0.087	(0.90 ± 1.5) × 10^{-7}	(6.5 ± 11) × 10^6	0.73 ± 0.033	this work
$F_1(\alpha R364K)$ (magnetic beads)	0.36 ± 0.14	(0.77 ± 1.2) × 10^{-6}	(1.5 ± 2.4) × 10^6	1.3 ± 0.049	19

[a]Determined from $3V_{max}/K_m$. [b]Determined from the distribution of dwell time of the catalytic pause. [c]The values are mean ± SD (standard deviation) of fitting. [d]Not determined.

DOI: 10.1021/bi501138b
Biochemistry 2015, 54, 472−480

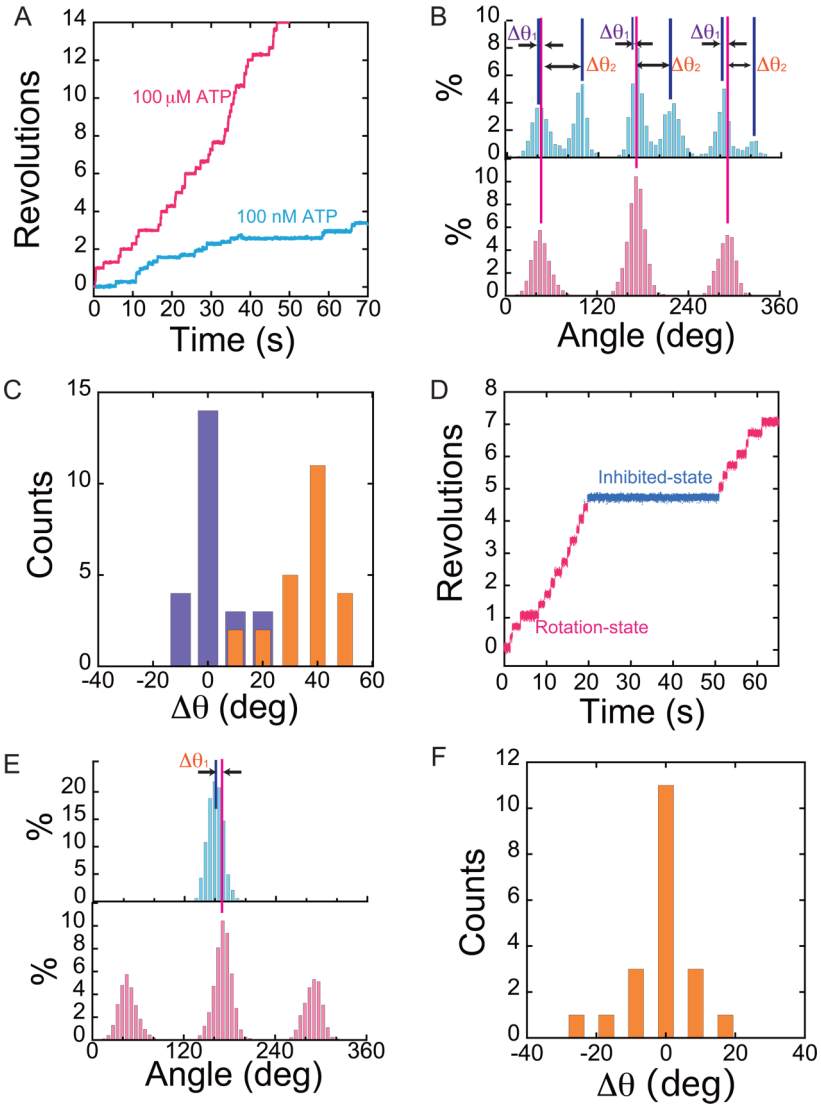

Figure 3. Identification of the pause angle of $F_1(\alpha$R364Lyk) at high ATP concentrations. A–C, rotation of $F_1(\alpha$R364Lyk) at different ATP concentrations. A, examples of time course of rotation. During observation, ATP concentration was changed from 100 μM ATP to 100 nM ATP. B, distributions of angle in the rotation. C, distributions of angular difference ($\Delta\theta_1$ or $\Delta\theta_2$ defined in B) between the pausing angles before and after buffer exchange. The averaged values of $\Delta\theta_1$ and $\Delta\theta_2$ are $-0.5 \pm 8.5°$ and $-39.2 \pm 11.1°$ (N = 24 and 4 molecules), respectively. D–F, inhibited states (long pauses) in the rotation of $F_1(\alpha$R364Lyk). D, example of time course of rotation containing a long pause. E, distributions of angle during long pause (top) and active rotation (bottom). F, distribution of angular difference ($\Delta\theta_1$ defined in E) between the angle of the short pause in active rotation and that of the long pause. The averaged value $\Delta\theta_1$ is $0.0 \pm 7.6°$ (N = 20 and 13 molecules). All measurements of D–F were carried out at 100 μM ATP.

5B). Thus, the stiffness and the torque showed a good correlation with each other.

Formation of Inhibited State. Unlike $F_1(\alpha$R364K) which tends to lapse into the severe ADP inhibited states, $F_1(\alpha$R364Lyk) mutant sustained successive rotation without frequently falling into the inhibited state (Figure 6A,B). Table 2 compares average durations of the rotating and inhibited states, $\tau^{rotating}$ and $\tau^{pausing}$, respectively, of the wild-type and the mutants. In the case of the wild-type, those states stay for similar durations of ~30 s, indicating that they have almost similar stability. The αR364K mutation shortens the duration of the rotating state by half and elongates that of the inhibited one by more than five times, giving rise to a decrease of $\tau^{rotating}/\tau^{pausing}$ by 1 order of magnitude which represents large reduction of activity due to enhanced formation of the inhibited state. The αR364A mutant also exhibits severe formation of the inhibited state, i.e., a decrease of $\tau^{rotating}/\tau^{pausing}$ by more than 2 orders of magnitude. On the other hand, the replacement of the Arg finger with Lyk increases and decreases $\tau^{rotating}$ and $\tau^{pausing}$, respectively, resulting in an increase of $\tau^{rotating}/\tau^{pausing}$ by a factor of 6.0 in comparison to that of the wild-type. The ratio $\tau^{rotating}/\tau^{pausing}$ of 6.0 indicates that the mutation stabilizes the rotating state by ~2 k_BT relative to the inhibited one and leads to significant improvement of avoidance of the inhibited-state formation even compared with the wild-type.

DISCUSSION

The measurements identified that the replacement of the Arg finger with Lyk makes an impact on the catalytic reaction step of ATP hydrolysis, whereas its effect on other steps, i.e., ATP binding and Pi release, remained minor. The stiffness and

DOI: 10.1021/bi501138b
Biochemistry 2015, 54, 472–480

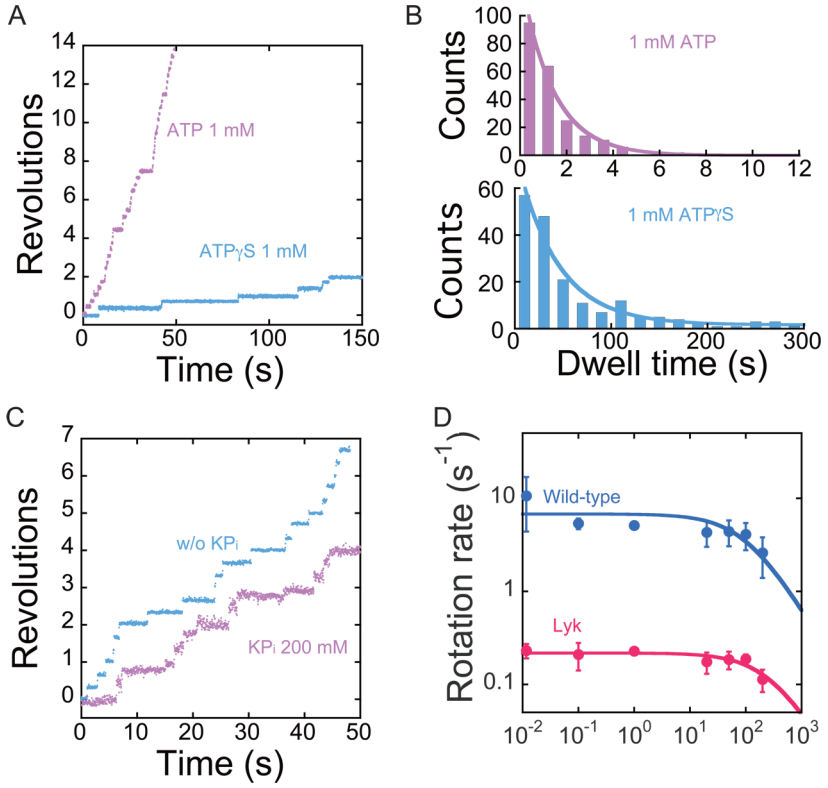

Figure 4. Identification of the elementary reaction step retarded in F_1(αR364Lyk) at high ATP concentrations. A and B, rotation of F_1(αR364Lyk) by ATPγS. A, examples of time course of rotation driven by 1 mM ATP (pearl pink) and 1 mM ATPγS (pearl blue). B, distributions of duration times of the pauses at 1 mM ATP (pearl purple, top) and 1 mM ATPγS (pearl blue, bottom). Solid lines show fit with the single-exponential decays with time constants of 1.4 s (ATP) and 42 s (ATPγS,) respectively. C and D, rotation of F_1(αR364Lyk) in the presence of excess P_i in solution. C, examples of time course of rotation at 1 mM ATP without P_i in solution (pearl blue) and with 200 mM P_i in solution (pearl purple). D, rotation rate at 1 mM ATP in the presence of various concentrations P_i in solution; the wild-type (blue) and F_1(αR364Lyk) (pink). The data were fitted with a curve according to a conventional competitive inhibition scheme: $v = (V_{max}[ATP])/([ATP] + K_m(1 + [P_i]/K_i))$, where K_i is the inhibitory constant. The determined values of the K_i for wild-type and F_1(αR364Lyk) were 1.2 and 0.25 mM, respectively.

torque measurements showed that the mutation affected the torque generation to some extent. The properties of F_1(αR364Lyk) mutant appear to be similar to those of F_1(αR364K) previously examined.[19] One exception, on the other hand, is the formation of the ADP inhibited state; F_1(αR364Lyk) mutant suppressed the formation of the inhibited state compared with F_1(αR364K) and even with the wild-type.

The Lyk mutation elongates the side-chain length of lysine and thus removes geometric mismatch between arginine and lysine residues at the Arg finger position in the wild-type F_1 and F_1(αR364K) mutant. The terminal amine group of Lyk is therefore geometrically accessible to the triphosphate moiety as in the wild-type F_1. Nevertheless, the catalytic activity of ATP hydrolysis of the Lyk mutant remained significantly lower than that of the wild-type and was not largely affected by the replacement of lysine with Lyk. The observation indicates that the geometric matching of the side-chain length is not a sole requirement for the Arg finger to catalyze the ATP hydrolysis reaction step, and detailed chemical properties of the terminal group that alter electrostatic interaction for the catalysis, in addition to simply carrying a positive charge, determine the Arg finger catalysis.

A clue to understand possible molecular properties that influence the catalytic reactivity is seen in an X-ray crystallographic structure[45] where the Arg finger undergoes large conformational changes and consequently is exposed into bulk water, instead of coordination to the substrate, in a prehydrolysis state. Because the Arg finger is located at the interface of the α and β subunits and the alkyl side chain of arginine is long and flexible, the terminal group is geometrically accessible to bulk water. The inhomogeneous conformations of the Arg finger observed in X-ray crystallographic structures[4,45] imply that stabilization of the coordination of the Arg finger to the substrate from the conformation in which the Arg finger is exposed into bulk water is moderate, and thus the proper catalytic coordination can be inhibited by perturbation due to changes in chemical properties of the terminal groups.

As described previously, the guanidinium ion of arginine possesses characteristic anisotropic properties of electrostatic interaction with its surroundings compared with the amine group of lysine and Lyk. The differences in electrostatic interaction are therefore expected to alter the stability of the catalytic coordination to the substrate. First, the extended distribution of the positive charge in the guanidinium group weakens solvation in bulk water, whereas the amine group with a localized positive charge exhibits a stronger solvation in bulk water. In addition, the guanidinium group of the Arg finger with the anisotropy of interaction due to the planarly extended conjugated structure, which gives rise to formation of a stable stacking pair of two guanidinium ions in water,[21−26] possibly favors the coordination to the substrate in the catalytic site more than the isotropic amine group since a guanidinium group of another arginine, βArg191 (βArg189 in MF_1), is situated

DOI: 10.1021/bi501138b
Biochemistry 2015, 54, 472−480

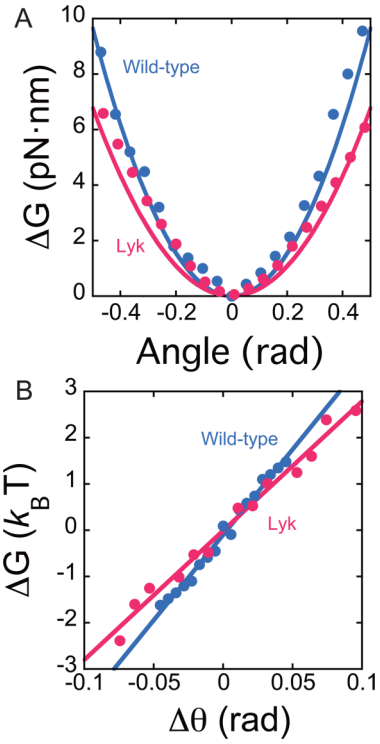

Figure 5. Rotary potential and rotary torque of wild-type and $F_1(\alpha R364Lyk)$. A, rotary potential in the catalytic pause of wild-type and $F_1(\alpha R364Lyk)$. The probability densities of angular position during the pause from the five molecules were transformed into rotary potential according to Bolzman's law: the wild-type (blue) and $F_1(\alpha R364Lyk)$ (pink). The determined potentials were well fitted with the harmonic functions; $\Delta G = 1/2\kappa\theta^2$, where κ is the stiffness. The determined values of κ were 79 and 54 pN·nm/rad for wild-type and $F_1(\alpha R364Lyk)$, respectively. B, torque determination of wild-type and $F_1(\alpha R364Lyk)$ using the fluctuation theorem. The $\ln[P(\Delta\theta)/P(-\Delta\theta)]$ is plotted against $\Delta\theta/k_BT$. The slope of this plot corresponds to the rotary torque generated by the wild-type (blue) and $F_1(\alpha R364Lyk)$ (pink). The average values of torque were determined from a linear fit of all data points (solid line). The values were 37 and 29 pN·nm for wild-type and $F_1(\alpha R364Lyk)$, respectively.

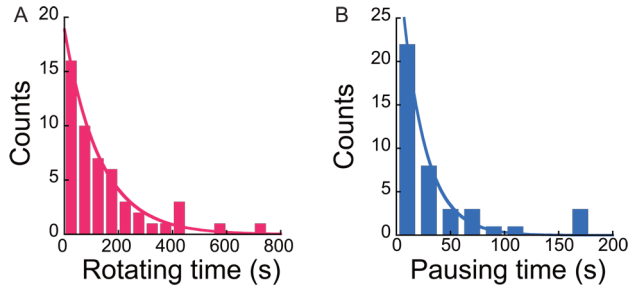

Figure 6. Analysis of inhibited states (long pauses) in the rotation of $F_1(\alpha R364Lyk)$. A, distribution of rotating times before lapsing into the long pause. B, distribution of pausing times before resuming the rotations. Each solid line shows the fit of the single-exponential decay function with a time constant of 132 ± 10 and 22 ± 2.0 s (mean ± SD), respectively.

next to that of the Arg finger in an approximate face-to-face alignment in the catalytic site as seen in X-ray crystallographic structures.[4] Finally, as also seen in X-ray crystallographic structures,[4] the branching two NH_2 moieties of the guanidinium group simultaneously recognize the β- and γ-phosphates of ATP, which should be absent in the case of the amine group. All of those factors of the Arg finger contribute to stabilization of its coordination to the substrate in the catalytic site relative to the conformation in which the side chain is exposed into bulk water, and lack of them in the Lyk mutant may hinder proper catalytic coordination of the amine group to the substrate. A possibility of such large conformational changes upon mutation of arginine to lysine due to the difference in solvation effect in cytochrome *c* has previously been proposed.[46] Although the electrostatic effect on catalysis in the preorganized binding site of protein has been well understood through theoretical analysis,[47] precise modeling of the preorganized binding structure upon the mutation that undergoes large conformational changes would be necessary for the prediction of the mutation effect.

Table 2. Average Duration of the Rotating State ($\tau^{rotating}$) and the Inhibited One ($\tau^{rotating}$) of Wild-Type, $F_1(\alpha R364K)$, $F_1(\alpha R364Lyk)$, and $F_1(\alpha R364A)$

sample	$\tau^{rotating}$ (s)	$\tau^{pausing}$ (s)	$\tau^{rotating}/\tau^{pausing}$	ref
wild-type	34	32.3	1.1	43
$F_1(\alpha R364Lyk)$	132	22	6.0	this work
$F_1(\alpha R364K)$	13	>180	<0.07	19
$F_1(\alpha R364A)$	2.3	>1000	<0.0023	40

There is also a possibility that the terminal amino group of Lyk is deprotonated since the protonation state of an amino group is not as stable as that of a terminal guanidinium group of arginine which possesses an extended π-conjugation. However, pK_a of a terminal amino group (pK_a = 11 in water solvent) is still generally much more stable than those of carboxyl groups, and only a few examples of pK_a modulation of a terminal amino group of lysine by four units have been found. As shown in an example of deprotonation of a lysine side chain found in a mutant of staphylococcal nuclease[48] where the deprotonated lysine is embedded in a hydrophobic core, the deprotonation would require a very hydrophobic environment. In the case of F_1-ATPase, on the other hand, the ATP binding site is very polar since the site accommodates triphosphate carrying charges of $-4e$. In fact, pK_a of Lyk in the binding pocket was empirically estimated to be 8.9 by PROPKA[49] (Yuko Ito, private communication). Considering the present experimental condition (pH 7) and the minor difference of pK_a between a guanidinium moiety (pK_a = 12) and a primary amine one, it is therefore unlikely that the terminal amine group of Lyk is deprotonated when it is coordinated to ATP.

The elongation of the side chain by the replacement of lysine with Lyk, on the other hand, diminished the severe inhibition even if the terminal group remained as amine. The observation is a clear indicative of importance of the geometric chain length matching, rather than chemical properties of the terminal groups, in the case of the inhibited-state formation. This phenomenon is consistent with the previous biochemical assay using the mutation of p-loop threonine to serine, where the chemical properties of the terminal groups were the same while the geometric chain length matching was modulated appropriately.[50] Substrate releases, which are presumably related to the inhibition process,[51,52] are thought to accompany rearrangement of the α–β interface that mediates the cooperative rotational catalysis among three catalytic sites. The fine-tuning of the chain length of the Arg finger may therefore be critical to controlling the inter-subunit conformational changes through interaction of the Arg finger. Moreover, the replacement of the

DOI: 10.1021/bi501138b
Biochemistry 2015, 54, 472–480

guanidinium group of the Arg finger with an amine in addition to the fine-tuning of the chain length in the mutation of F_1(αR364Lyk) stabilizes the rotating state relative to the inhibited state in comparison with the wild-type, indicating that strong interaction of the terminal group at the position of the Arg finger with the substrate plays an essential role in the functional cooperativity.

The present study demonstrated that the use of an unnatural amino acid, Lyk, allows one to finely resolve chemical factors of the Arg finger that determine the ATPase activity of F_1-ATPase. We elucidated that the geometric chain length matching is not a sole determinant for the catalytic reaction and characteristic chemical properties of the terminal guanidinium group of arginine are crucial for the Arg finger catalysis through electrostatic interaction. The planar anisotropic chemical structure of the guanidinium group is suggested to facilitate proper catalytic coordination of the Arg finger to the substrate. The geometric chain length matching restored by the Lyk mutation was, on the other hand, found to prevent frequent formation of the inhibited state, which is presumably related to ligand release processes, observed in the lysine mutant. Moreover, stronger interaction of the terminal group fulfilled by the Lyk mutation was shown to stabilize the rotating state and thus improve avoidance of the inhibited-state formation even compared with the wild-type. Those chemical insights into the role of the functionally important amino acid residue were successfully obtained by the chemical modification of structure precisely designed beyond mutation with natural amino acids in a conventional biochemical approach. In addition, the functional improvement over the wild-type was attained with the small but finely determined chemical modification. Incorporation of unnatural amino acids will be a new research strategy widely extending with its high "chemical" resolution biochemical approaches for elucidation of the molecular mechanism of protein functions as well as engineering for gain-of-function.

■ ASSOCIATED CONTENT

Supporting Information

Preparation of the mutant α(His_6 at N-terminus/FLAG-tag at C-terminus/C193S/R364Lyk) subunit (αR364Lyk). This material is available free of charge via the Internet at http://pubs.acs.org.

■ AUTHOR INFORMATION

Corresponding Author

*Tel.: +81-3-5841-7252. Fax: +81-3-5841-1872. E-mail: hnoji@appchem.t.u-tokyo.ac.jp.

Author Contributions

A.Y. designed and performed the experiments and analyzed the data; R.I., R.W., and S.H. gave technical support and conceptual advice; H.N. designed the experiments, built the whole story, and wrote the paper with A.Y., R.I., R.W., and S.H.

Funding

This work was supported in part by Grants-in-Aid for Scientific Research (18074005 to H.N. and 24651167 to R.I.) from the Ministry of Education, Culture, Sports, Science and Technology, Japan.

Notes

The authors declare no competing financial interest.

■ ACKNOWLEDGMENTS

We thank Yuko Ito for pK_a calculation of Lyk, Rie Iino for technical help, and all of the members of the Noji laboratory for valuable discussions and advice. S.H. also thanks Taichi Inagaki and Takeshi Yamamoto for valuable comments.

■ ABBREVIATIONS

F_1, F_1-ATPase; TF_1, F_1-ATPase from thermophilic *Bacillus* PS3; MF_1, F_1-ATPase from bovine or yeast mitochondria; ATPγS, adenosine 5-[γ-thio]triphosphate.

■ REFERENCES

(1) Ahmadian, M. R., Stege, P., Scheffzek, K., and Wittinghofer, A. (1997) Confirmation of the arginine-finger hypothesis for the GAP-stimulated GTP-hydrolysis reaction of Ras. *Nat. Struct. Biol. 4*, 686−689.

(2) Scheffzek, K., Ahmadian, M. R., Kabsch, W., Wiesmuller, L., Lautwein, A., Schmitz, F., and Wittinghofer, A. (1997) The Ras-RasGAP complex: structural basis for GTPase activation and its loss in oncogenic Ras mutants. *Science 277*, 333−338.

(3) Suno, R., Niwa, H., Tsuchiya, D., Zhang, X., Yoshida, M., and Morikawa, K. (2006) Structure of the whole cytosolic region of ATP-dependent protease FtsH. *Mol. Cell 22*, 575−585.

(4) Abrahams, J. P., Leslie, A. G., Lutter, R., and Walker, J. E. (1994) Structure at 2.8 A resolution of F_1-ATPase from bovine heart mitochondria. *Nature 370*, 621−628.

(5) Le, N. P., Omote, H., Wada, Y., Al-Shawi, M. K., Nakamoto, R. K., and Futai, M. (2000) Escherichia coli ATP synthase alpha subunit Arg-376: the catalytic site arginine does not participate in the hydrolysis/synthesis reaction but is required for promotion to the steady state. *Biochemistry 39*, 2778−2783.

(6) Soga, S., Noumi, T., Takeyama, M., Maeda, M., and Futai, M. (1989) Mutational replacements of conserved amino acid residues in the alpha subunit change the catalytic properties of Escherichia coli F_1-ATPase. *Arch. Biochem. Biophys. 268*, 643−648.

(7) Nadanaciva, S., Weber, J., Wilke-Mounts, S., and Senior, A. E. (1999) Importance of F_1-ATPase residue αArg-376 for catalytic transition state stabilization. *Biochemistry 38*, 15493−15499.

(8) Baker, T. A., and Sauer, R. T. (2012) ClpXP, an ATP-powered unfolding and protein-degradation machine. *Biochim. Biophys. Acta 1823*, 15−28.

(9) Enemark, E. J., and Joshua-Tor, L. (2008) On helicases and other motor proteins. *Curr. Opin. Struct. Biol. 18*, 243−257.

(10) Iino, R., and Noji, H. (2013) Intersubunit coordination and cooperativity in ring-shaped NTPases. *Curr. Opin. Struct. Biol. 23*, 229−234.

(11) Cox, J. M., Abbott, S. N., Chitteni-Pattu, S., Inman, R. B., and Cox, M. M. (2006) Complementation of one RecA protein point mutation by another - Evidence for trans catalysis of ATP hydrolysis. *J. Biol. Chem. 281*, 12968−12975.

(12) Cox, J. M., Li, H., Wood, E. A., Chitteni-Pattu, S., Inman, R. B., and Cox, M. M. (2008) Defective dissociation of a "Slow" RecA mutant protein imparts an Escherichia coli growth defect. *J. Biol. Chem. 283*, 24909−24921.

(13) Glennon, T. M., Villa, J., and Warshel, A. (2000) How does GAP catalyze the GTPase reaction of Ras?: A computer simulation study. *Biochemistry 39*, 9641−9651.

(14) Dittrich, M., Hayashi, S., and Schulten, K. (2003) On the mechanism of ATP hydrolysis in F_1-ATPase. *Biophys. J 85*, 2253−2266.

(15) Hayashi, S., Ueno, H., Shaikh, A. R., Umemura, M., Kamiya, M., Ito, Y., Ikeguchi, M., Komoriya, Y., Iino, R., and Noji, H. (2012) Molecular mechanism of ATP hydrolysis in F_1-ATPase revealed by molecular simulations and single-molecule observations. *J. Am. Chem. Soc. 134*, 8447−8454.

DOI: 10.1021/bi501138b
Biochemistry 2015, 54, 472−480

(16) Yang, W., Gao, Y. Q., Cui, Q., Ma, J., and Karplus, M. (2003) The missing link between thermodynamics and structure in F_1-ATPase. *Proc. Natl. Acad. Sci. U.S.A. 100*, 874−879.
(17) Shurki, A., and Warshel, A. (2004) Why does the Ras switch "break" by oncogenic mutations? *Proteins 55*, 1−10.
(18) Kamerlin, S. C. L., Sharma, P. K., Prasad, R. B., and Warshel, A. (2013) Why nature really chose phosphate. *Q. Rev. Biophys. 46*, 1−132.
(19) Komoriya, Y., Ariga, T., Iino, R., Imamura, H., Okuno, D., and Noji, H. (2012) Principal role of the arginine finger in rotary catalysis of F_1-ATPase. *J. Biol. Chem. 287*, 15134−15142.
(20) Kagawa, R., Montgomery, M. G., Braig, K., Leslie, A. G., and Walker, J. E. (2004) The structure of bovine F_1-ATPase inhibited by ADP and beryllium fluoride. *EMBO J. 23*, 2734−2744.
(21) Boudon, S., Wipff, G., and Maigret, B. (1990) Monte-Carlo Simulations on the Like-Charged Guanidinium Guanidinium Ion-Pair in Water. *J. Phys. Chem 94*, 6056−6061.
(22) Soetens, J. C., Millot, C., Chipot, C., Jansen, G., Angyan, J. G., and Maigret, B. (1997) Effect of polarizability on the potential of mean force of two cations. The guanidinium-guanidinium ion pair in water. *J. Phys. Chem. B 101*, 10910−10917.
(23) No, K. T., Nam, K. Y., and Scheraga, H. A. (1997) Stability of like and oppositely charged organic ion pairs in aqueous solution. *J. Am. Chem. Soc. 119*, 12917−12922.
(24) Mason, P. E., Neilson, G. W., Enderby, J. E., Saboungi, M. L., Dempsey, C. E., MacKerell, A. D., and Brady, J. W. (2004) The structure of aqueous guanidinium chloride solutions. *J. Am. Chem. Soc. 126*, 11462−11470.
(25) Kubickova, A., Krizek, T., Coufal, P., Wernersson, E., Heyda, J., and Jungwirth, P. (2011) Guanidinium Cations Pair with Positively Charged Arginine Side Chains in Water. *J. Phys. Chem. Lett. 2*, 1387−1389.
(26) Shih, O., England, A. H., Dallinger, G. C., Smith, J. W., Duffey, K. C., Cohen, R. C., Prendergast, D., and Saykally, R. J. (2013) Cation-cation contact pairing in water: Guanidinium. *J. Chem. Phys. 139*, No. 035104.
(27) Neves, M. A. C., Yeager, M., and Abagyan, R. (2012) Unusual Arginine Formations in Protein Function and Assembly: Rings, Strings, and Stacks. *J. Phys. Chem. B 116*, 7006−7013.
(28) Yasuda, R., Noji, H., Yoshida, M., Kinosita, K., Jr., and Itoh, H. (2001) Resolution of distinct rotational substeps by submillisecond kinetic analysis of F_1-ATPase. *Nature 410*, 898−904.
(29) Weber, J. (2010) Structural biology: Toward the ATP synthase mechanism. *Nat. Chem. Biol. 6*, 794−795.
(30) Junge, W., Sielaff, H., and Engelbrecht, S. (2009) Torque generation and elastic power transmission in the rotary F_oF_1-ATPase. *Nature 459*, 364−370.
(31) Noji, H., Yasuda, R., Yoshida, M., and Kinosita, K., Jr. (1997) Direct observation of the rotation of F_1-ATPase. *Nature 386*, 299−302.
(32) Kabaleeswaran, V., Puri, N., Walker, J. E., Leslie, A. G., and Mueller, D. M. (2006) Novel features of the rotary catalytic mechanism revealed in the structure of yeast F_1 ATPase. *EMBO J. 25*, 5433−5442.
(33) Cingolani, G., and Duncan, T. M. (2011) Structure of the ATP synthase catalytic complex (F_1) from Escherichia coli in an autoinhibited conformation. *Nat. Struct. Mol. Biol. 18*, 701−707.
(34) Spetzler, D., Ishmukhametov, R., Hornung, T., Day, L. J., Martin, J., and Frasch, W. D. (2009) Single molecule measurements of F_1-ATPase reveal an interdependence between the power stroke and the dwell duration. *Biochemistry 48*, 7979−7985.
(35) Sielaff, H., Rennekamp, H., Wachter, A., Xie, H., Hilbers, F., Feldbauer, K., Dunn, S. D., Engelbrecht, S., and Junge, W. (2008) Domain compliance and elastic power transmission in rotary F_oF_1-ATPase. *Proc. Natl. Acad. Sci. U.S.A. 105*, 17760−17765.
(36) Bilyard, T., Nakanishi-Matsui, M., Steel, B. C., Pilizota, T., Nord, A. L., Hosokawa, H., Futai, M., and Berry, R. M. (2013) High-resolution single-molecule characterization of the enzymatic states in Escherichia coli F_1-ATPase. *Philos. Trans. R. Soc. London, Ser. B: Biol. Sci. 368*, 20120023.
(37) Al-Hallaq, R. A., Yasuda, R. P., and Wolfe, B. B. (2001) Enrichment of N-methyl-D-aspartate NR1 splice variants and synaptic proteins in rat postsynaptic densities. *J. Neurochem. 77*, 110−119.
(38) Dunah, A. W., Luo, J., Wang, Y. H., Yasuda, R. P., and Wolfe, B. B. (1998) Subunit composition of N-methyl-D-aspartate receptors in the central nervous system that contain the NR2D subunit. *Mol. Pharmacol. 53*, 429−437.
(39) Hayashi, K., Ueno, H., Iino, R., and Noji, H. (2010) Fluctuation theorem applied to F_1-ATPase. *Phys. Rev. Lett. 104*, No. 218103.
(40) Watanabe, R., Matsukage, Y., Yukawa, A., Tabata, K. V., and Noji, H. (2014) Robustness of the Rotary Catalysis Mechanism of F_1-ATPase. *J. Biol. Chem. 289*, 19331−19340.
(41) Rondelez, Y., Tresset, G., Nakashima, T., Kato-Yamada, Y., Fujita, H., Takeuchi, S., and Noji, H. (2005) Highly coupled ATP synthesis by F_1-ATPase single molecules. *Nature 433*, 773−777.
(42) Watanabe, R., Iino, R., and Noji, H. (2010) Phosphate release in F_1-ATPase catalytic cycle follows ADP release. *Nat. Chem. Biol. 6*, 814−820.
(43) Hirono-Hara, Y., Noji, H., Nishiura, M., Muneyuki, E., Hara, K. Y., Yasuda, R., Kinosita, K., Jr., and Yoshida, M. (2001) Pause and rotation of F_1-ATPase during catalysis. *Proc. Natl. Acad. Sci. U.S.A. 98*, 13649−13654.
(44) Shimabukuro, K., Yasuda, R., Muneyuki, E., Hara, K. Y., Kinosita, K., Jr., and Yoshida, M. (2003) Catalysis and rotation of F_1 motor: cleavage of ATP at the catalytic site occurs in 1 ms before 40 degree substep rotation. *Proc. Natl. Acad. Sci. U.S.A. 100*, 14731−14736.
(45) Gibbons, C., Montgomery, M. G., Leslie, A. G. W., and Walker, J. E. (2000) The structure of the central stalk in bovine F_1-ATPase at 2.4 angstrom resolution. *Nat. Struct. Biol. 7*, 1055−1061.
(46) Cutler, R. L., Davies, A. M., Creighton, S., Warshel, A., Moore, G. R., Smith, M., and Mauk, A. G. (1989) Role of Arginine-38 in Regulation of the Cytochrome-C Oxidation-Reduction Equilibrium. *Biochemistry 28*, 3188−3197.
(47) Warshel, A., Sharma, P. K., Chu, Z. T., and Aqvist, J. (2007) Electrostatic contributions to binding of transition state analogues can be very different from the corresponding contributions to catalysis: Phenolates binding to the oxyanion hole of ketosteroid isomerase. *Biochemistry 46*, 1466−1476.
(48) Takayama, Y., Castaneda, C. A., Chimenti, M., Garcia-Moreno, B., and Iwahara, J. (2008) Direct evidence for deprotonation of a lysine side chain buried in the hydrophobic core of a protein. *J. Am. Chem. Soc. 130*, 6714−6715.
(49) Sondergaard, C. R., Olsson, M. H. M., Rostkowski, M., and Jensen, J. H. (2011) Improved Treatment of Ligands and Coupling Effects in Empirical Calculation and Rationalization of pK_a Values. *J. Chem. Theory Comput. 7*, 2284−2295.
(50) Jault, J. M., Dou, C., Grodsky, N. B., Matsui, T., Yoshida, M., and Allison, W. S. (1996) The $\alpha_3\beta_3\gamma$ subcomplex of the F_1-ATPase from the thermophilic Bacillus PS3 with the βT165S substitution does not entrap inhibitory MgADP in a catalytic site during turnover. *J. Biol. Chem. 271*, 28818−28824.
(51) Mitome, N., Ono, S., Suzuki, T., Shimabukuro, K., Muneyuki, E., and Yoshida, M. (2002) The presence of phosphate at a catalytic site suppresses the formation of the MgADP-inhibited form of F_1-ATPase. *Eur. J. Biochem. 269*, 53−60.
(52) Watanabe, R., and Noji, H. (2014) Timing of inorganic phosphate release modulates the catalytic activity of ATP-driven rotary motor protein. *Nat. Commun. 5*, No. 3486.
(53) Tanigawara, M., Tabata, K. V., Ito, Y., Ito, J., Watanabe, R., Ueno, H., Ikeguchi, M., and Noji, H. (2012) Role of the DELSEED loop in torque transmission of F_1-ATPase. *Biophys. J 103*, 970−978.

DOI: 10.1021/bi501138b
Biochemistry 2015, 54, 472−480